Modelling the Localization Error of an AoA-based Localization System

Francesco Furfari, Paolo Barsocchi, Michele Girolami and Fabio Mavilia
Italian National Council of Research, ISTI-CNR, Pisa, Italy
Email: {name.surname}@isti.cnr.it

***Abstract*—Indoor localization provides important context information to develop Intelligent Environments able to understand user situations, to react and adapt to changes in the surrounding environment. Bluetooth 5.1 Direction Finding (DF) is a recent specification based on angle of departure (AoD) and arrival (AoA) of radio signals and it is addressed to localize objects or people in indoor scenarios. In this work, we study the error propagation of an indoor localization system based on AoA technique and on multiple anchor receivers.**

***Index Terms*—Bluetooth 5.1, Direction Finding, Angle of Arrival, Indoor Localization**

I. Introduction

Indoor localization techniques have rapidly increased their accuracy and availability in the last decade, as many IoT scenarios require the existence of a location-based service estimating the location. The technological trend is moving toward the adoption of RF-based technologies [1], combined with the use of different techniques, such as RSS (Received Signal Strength), AoA or AoD (Angle of Arrival and Departure), PDoA (Phase Difference of Arrival) and ToF (Time of Flight). Under this respect, the use of short-range wireless technologies, such as Bluetooth, WiFi and Ultra Wide Band (UWB) plays a crucial role. In 2019, the Bluetooth SIG (Special Interest Group) delivered a new protocol specification, in extension to the Bluetooth Core Specification 5.1, named Bluetooth 5.1 Direction Finding (DF) [2]. The DF specification is based on AoD and AoA techniques and it is oriented to the indoor positioning of objects and people. The receiving device, e.g. an anchor deployed in an indoor environment, is basically equipped with an antenna array and a micro-controller measuring the phase difference of messages sent by a tag [3]. The tag advertises BLE beacons with an additional field that follows the CRC code, namely Constant Tone Extension (CTE). The CTE consists of a RF sinusoidal signal modulated by a constant series of consecutive ones. Throughout the CTE part of the BLE packet and by knowing wavelength λ of the signal and the distance d between the antennas, the receiver is able to calculate the angle-of-arrival of the signal.

In this work, we study the characteristics of BT5.1 Direction Finding (AoA) starting from the differences and similarities with the commonly adopted RSSI-based trilateration. In particular, we measure the confidence region resulting from a trilateration-based approach and we study how such region extends or contracts by varying: the antenna's locations, the distance and the angle between the emitting device (e.g. the Bluetooth tag) and the antennas. We describe our simulation tool calibrated according to our previous data collection campaign [4]. The resulting confidence regions enable to easily understand the optimal locations of 2 antennas in a wide indoor room and to understand the limits of an AoA-based localization technique.

II. Characterizing the Localization Error

Trilateration is a mathematical technique estimating the position of a target, i.e. an object based on three landmarks. In the case of the RSSI (Received Signal Strength Indicator) value, it is possible to estimate the distance d_{rssi} between an emitter and a receiver with the use of an indoor propagation model. In turn, by using 3 anchor nodes, it is theoretically possible to estimate the target location with a trilateration approach. Trilateration consists of intersecting the circles centered in the anchor's locations of radius d_{rssi}, obtained by converting the RSSI value with a distance measure. However, in real settings, several issues have to be considered. The first and most common issue is that circles may not intersect, as the radius d_{rssi} is highly affected by the highly variability of the RSSI value. If the distance is underestimated, then circles may not intersect at all. Generally, the intersection of circles brings to curved triangles whose barycenter is taken as target estimation, and curved triangle represents the confidence region for the measurement, as reported in Fig. 1. The Bluetooth DF specification allows estimating the angle

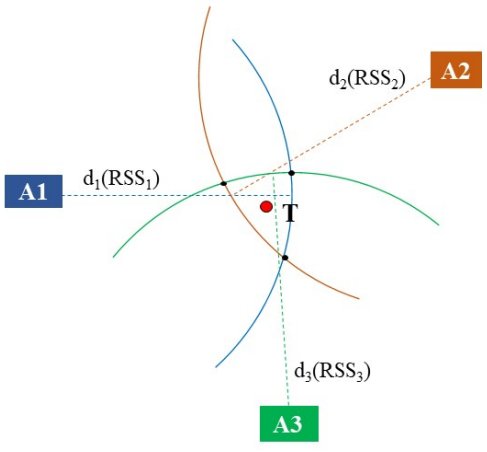

Fig. 1: Position estimation with RSSI-based trilateration.

of the signal received by an emitter and a receiver with two

angles: the azimuth and the elevation angles. Differently from RSSI-based trilateration, in the case of AoA it is no longer required the use 3 anchor nodes to detect the target's position. More specifically, if the target's height h is known, then the planar coordinates of the target can be estimated with one anchor. In this case, it is possible to intersect the cone generated by the elevation angle with a plane orthogonal to the azimuth plane along the azimuth direction [4]. Differently, if target's h height is unknown, then two anchors are required to estimate the target's position. In particular, the estimated position T can be simply calculated by intersecting the straight lines representing the azimuth directions.

We focus on this second case, and we report in Fig.2 the location of 2 anchors A1 and A2 orthogonally placed on the adjacent walls. The azimuth angles range from $-90°$ to $+90°$ (left to right in Fig. 2), then the linear equations of the directions provided by the 2 anchors are given by:

$$\begin{cases} \tan(\phi_1) \cdot x + y = y_{a1} \\ -\cot(\phi_2) \cdot x + y = -\cot(\phi_2) \cdot x_{a2} \end{cases} \quad (1)$$

whose solution can be obtained with the Cramer's rule as follows:

$$x_T = \frac{D_x}{D} = \frac{y_{a1} + \cot(\phi_2) \cdot x_{a2}}{\tan(\phi_1) + \cot(\phi_2)}; \quad (2)$$

$$y_T = \frac{D_y}{D} = \frac{\cot(\phi_2) \cdot (y_{a1} - \tan(\phi_1) \cdot x_{a2})}{\tan(\phi_1) + \cot(\phi_2)} \quad (3)$$

Nevertheless, some corner cases limit the usability of Equations 2 and 3. In particular, when the system is indeterminate, that's the determinants D, D_x, D_y are equal to 0, the directions detected by the anchors are parallel and coincident as shown in Fig. 3.a. It may occur when the target's location (reported as the red circle in Fig. 3) is somewhere along the segment joining the two anchors. Another corner case occurs when the directions are parallel but not coincident, as reported in Fig. 3.b. As for example, $D = 0$, and $D_x \neq 0$ or $D_y \neq 0$, in this case no valid solutions for Equations 2 and 3 exist. A possible alternative is to use a third anchor node in order to add 1 extra equation to the linear system reported in Equation 1. A further corner case is when there are valid intersections, that is $D \neq 0$, but the estimated target's location falls outside the indoor environment. In Fig. 3.c we report this situation, in which the anchors measure slightly different directions to the target and the resulting intersection falls beyond the walls of the room. Such a situation can be easily resolved by intersecting the lines with the boundaries of the environment. Finally, the last corner case we consider is represented in Fig. 3.d. In this case, the target is still along the line joining the 2 anchors, and small measurement errors can be amplified to project the intersection of lines very far from the target (red square in Fig. 3.d).

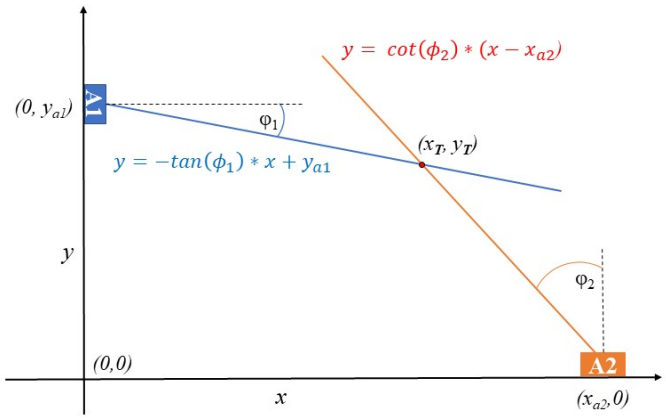

Fig. 2: Position estimation using azimuth angles.

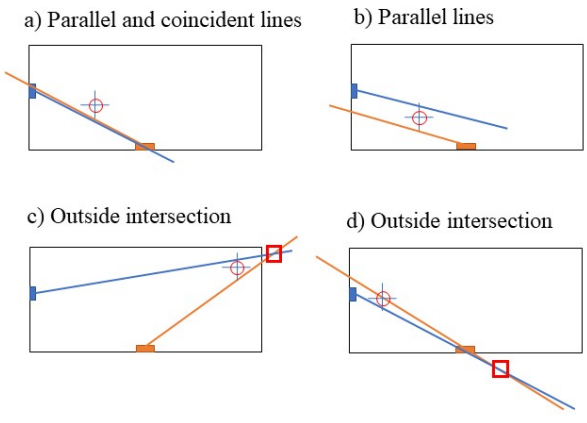

Fig. 3: Special cases with direction finding.

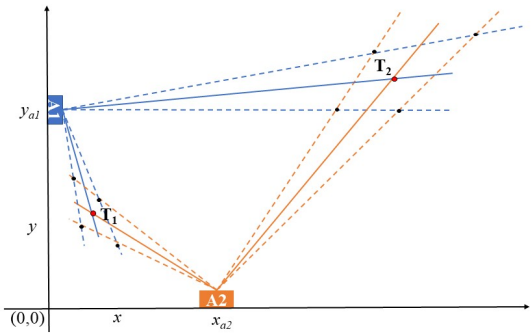

Fig. 4: Size of confidence regions depends on target position.

III. Modelling the Localization Area

We now focus on how to determine the confidence region for the target's location. To this purpose, we consider the average error of the estimated angles between anchors and the target. In Fig. 4 we represent 2 targets, T1 and T2, with the corresponding confidence regions. In this case, we consider $5°$ of absolute error [1], to the target locations in order to get boundaries directions for each measurement. The confidence region is represented by the polygons obtained by intersecting

[1] As reported with the ublox XPLR-AOA datasheet

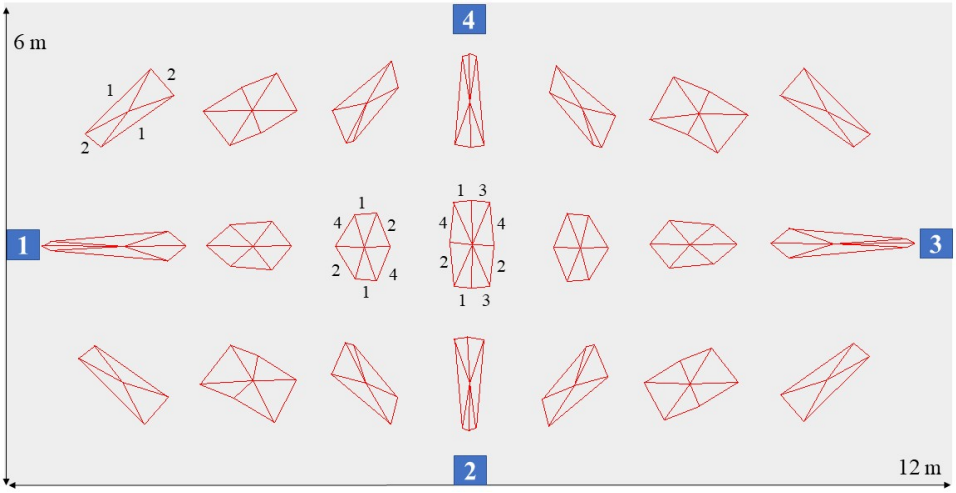

Fig. 5: Confidence regions in different positions of a room setting with 4 anchors.

4 boundaries directions (represented as dotted lines in Fig. 4) and the max distance error is determined by the greater polygons' diagonal. From Fig. 4, it is possible to notice that the area of the confidence regions depends on the target location. In the case of the target's locations close to the anchor locations (T_1 in figure), the max error distance is low, far away from the anchors the lozenge is deformed and error distance amplified (T_2). It is, therefore, reasonable to ask what is the average area and distance error of the confidence regions in a given setting. Furthermore, is it possible to reduce the distance error by adding anchors to the setting?

A. The Simulation Tool

In order to address the previously stated research questions, we developed a simulation tool which allows to place anchors arbitrarily and calculate the resulting confidence regions. The tool also considers the dimension of the indoor environment, e.g. a $12m \times 6m$ room in which we placed 4 anchors, one for each room's side. The simulator considers the equations described in (1) one for each of the 4 anchors, resulting with 6 different linear systems which can determine 6 points of intersection. In turn, the simulator considers as target's locations the resulting center of gravity. Similarly, the confidence regions can be obtained as the intersection of the various polygons obtained by the linear systems of the boundaries directions. In Fig. 5, we show 21 confidence regions obtained with the previously described method. The anchors (blue boxes) are placed in the middle of each room side. The shape of the regions are now polygons of different shapes of increasing complexity ranging from quadrilaterals and octagons. The numbers shown on the edges of three polygons in the Fig. 5 indicate which anchor contributes to forming the side of the polygon. It should be noted that in the center of the room, the shape of the confidence region is an octagon as it is obtained with the contribution of all 4 anchors. Instead, the shape of the next region on the left side is a hexagon whose sides are determined by 3 anchors, and finally, on the top left of Fig. 5 we have a quadrilateral defined by only 2 anchors. We observe that anchor 3, placed on the right wall, fails to add relevant information for the positions that are more than half of the room. The boundaries directions of anchor 3 beyond 6 meters are too wide and cannot further limit the areas obtained from the intersection of the other border directions. It is important to note that for the quadrilateral highlighted in the upper left corner, also the contribution of anchor 4 is no longer necessary. If during the estimation of the position, we avoided using the information provided by anchor 4, we would avoid running into the problems highlighted in Fig. 3.d, i.e. that the intersections with anchor 4 strongly unbalance the center of gravity of the estimated position.

The simulator computes various information related to the confidence region: the area, the maximum and minimum distance error, and the target's position providing the maximums and minimum errors. Table I shows some information computed by our simulator, as the position of the anchors on the long side of the room varies. Given the symmetry of the considered problem, we decided to move the anchors in a mirror way, starting from the ends of the room, with anchor 2 positioned to the left ($X_{A2} = 1m$) and anchor 4 positioned to the right ($X_{A4} = 11m$), and bring them closer towards the center by moving them 1 meter at a time until both are positioned at 6 meters. For each movement of the anchors, 189 confidence regions of different positions were calculated, starting at 1 meter from the anchors and 50 cm apart from each other. From the simulation results reported in Table I, we observe that with a uniform error distribution of $5°$ for the azimuth angle, we obtain $59cm$ as the lowest mean error of the distances. Such result is obtained when the 4 anchors are positioned with the following anchor's layout: $X_{A2} = 6m; X_{A4} = 6m$. Differently, if the goal is minimizing the maximum error, then the optimal anchor's locations is given by $X_{A2} = 5m; X_{A4} = 7m$ resulting with $0.85m$. We further analyze the metrics reported in Table I, by varying the error introduced during the angle estimating on the azimuth

Az. Err	Mean dist.	Min dist.	Max dist.	X_{A2}	X_{A4}
5° uniform	0.93	**0.28**	1.69	1.00	11.00
	0.79	0.32	1.39	2.00	10.00
	0.69	0.37	1.08	3.00	9.00
	0.63	0.44	0.93	4.00	8.00
	0.60	0.41	**0.85**	5.00	7.00
	0.59	0.40	1.00	**6.00**	**6.00**

TABLE I: Summary of position errors moving anchors on long side, assuming constant error in bearing azimuth angles

Az. Err	Mean dist.	Min dist.	Max dist.	X_{A2}	X_{A4}
5° up to 25°	2.83	**0.28**	4,81	1.00	11.00
	2.33	0.34	4.03	2.00	10.00
	1.91	0.47	3.10	3.00	9.00
	1.83	0.67	3.20	**4.00**	**8.00**
	1.90	0.96	3.03	5.00	7.00
	1.98	0.99	**3.00**	6.00	6.00

TABLE II: Summary of position errors moving anchors assuming increasing error in bearing azimuth angles.

plane in the range 5° to 25°, as reported in Table II. According to these settings, the lowest mean error is obtained with a different anchor's layout: ($X_{A2} = 4m; X_{A4} = 8m$) and the average error is, of course, greater: $1.83m$.

B. Experimental Results with Azimuth Error Analysis

A detailed study of azimuth errors for a single anchor is reported in [4]. Real data are collected by using the XPLR-AOA[2] kit produced by ublox, compliant with BT5.1 DF specifications. In [4] the ground truth, that is the expected azimuth (ϕ) and elevation (δ) angle for the 28 marked locations are compared to the anchor's estimated angles ($\hat{\phi}$, $\hat{\delta}$). The

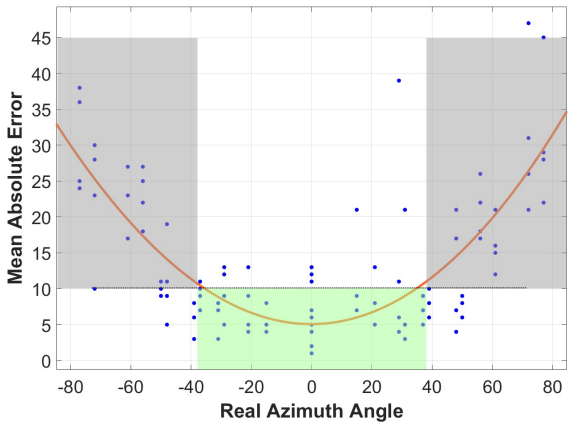

Fig. 6: MAE_ϕ varying the real azimuth angle for the 28 locations.

mean absolute error (MAE) between the real azimuth angles and the estimated ones is calculated as follows: $MAE_\phi = \frac{\sum_{i=1}^{n} |\phi_i - \hat{\phi}_i|}{n}$. In Fig. 6, we report with blue dots the MAE_ϕ by varying the real azimuth angle for the 28 locations. The fitting orange curve in Fig. 6 is well featured by a quadratic model, in the form of $f(x) = p_1 \cdot x^2 + p_2 \cdot x + p_3$. The coefficients of the second degree polynomial we obtain are: $p_1 = 0.004$, $p_2 = 0.00586$, $p_3 = 5.08$. Setting an angle error threshold of 10°, the curve satisfies the threshold in the range $-40° \leq \phi \leq 40°$ (green area), while it exceeds such limit for the rest of the interval, reaching errors of 30°(the grey areas in Fig. 6). As a general trend, the AoA error does not only depend on the distance from the anchor, but also on how much the target location is in a peripheral area i.e. outside of the green region. Although the error model used in the simulator (set to 5°) is declared by the manufacturer, many considerations on the confidence regions remain valid, and by replacing the model with the one obtained with a measurement campaign, it is possible to obtain qualitative evaluations for the placement of the anchors. The shape of the confidence regions changes to irregular polygons, but it is always possible to determine the contribution of an anchor in the position estimation.

[2]https://www.u-blox.com/en/product/xplr-aoa-1-kit

IV. Conclusions and Future Directions

Localizing a user in an indoor environment is one of the main building blocks of any intelligent environment. It is, indeed, essential to understand user situations and to react and adapt to changes in the surrounding environment. Therefore, analysing the optimal placement of BT5.1 Direction Finding anchors to minimize indoor localization error, plays a crucial role. For this reason, we developed a tool that, calibrated with real data collected through an experimental campaign, is able to define confidence accuracy regions. We plan to organize a more extended data collection campaign through which collect useful data to better characterize the error of the estimated angles with respect to the ground truth at realistic conditions. Moreover, we plan to analyse how the mean absolute error changes with the distance between anchors and target's location. We expect to exploit the collected dataset to validate the proposed simulation tool.

Acknowledgment

This work is partially supported by the ChAALenge project (B89J22002310005) and PNRR-PE8 AGE-IT project (B83C22004880006).

References

[1] F. Potortì, A. Crivello, F. Palumbo, M. Girolami, and P. Barsocchi, "Trends in smartphone-based indoor localisation," in *2021 International Conference on Indoor Positioning and Indoor Navigation (IPIN)*. IEEE, 2021, pp. 1–7.

[2] "Bluetooth Special Interest Group (SIG). Bluetooth 5.1 Direction Finding," Tech. Rep., 2019. [Online]. Available: https://www.bluetooth.com/wp-content/uploads/2019/05/BTAsia/1145-NORDIC-Bluetooth-Asia-2019Bluetooth-5.1-Direction-Finding-Theory-and-Practice-v0.pdf

[3] G. Pau, F. Arena, Y. E. Gebremariam, and I. You, "Bluetooth 5.1: An analysis of direction finding capability for high-precision location services," *Sensors*, vol. 21, no. 11, 2021.

[4] M. Girolami, P. Barsocchi, F. Furfari, D. La Rosa, and F. Mavilia, "Evaluation of angle of arrival in indoor environments with bluetooth 5.1 direction finding," in *2022 18th International Conference on Wireless and Mobile Computing, Networking and Communications (WiMob)*, 2022, pp. 284–289.